Electrical Properties Of Li And Nd Doped Srbi$_4$ti$_4$o$_{15}$ Ceramics

K. Ashok[1], M. Buchi Suresh[2] and P. Sarah[1*]
[1]Material Research Lab, Vardhaman College of Engineering, Hyderabad-501218, A.P, India
[2]ARCI, Balapur, Hyderabad-500005, A.P, India

Abstract: Ceramic samples of $Sr_{0.2}Li_{0.4}Nd_{0.4}Bi_4Ti_4O_{15}$ (SLNBT) are prepared by high temperature solid state reaction method with a view to study their electrical properties by Complex Impedance Spectroscopy (CIS). Nyquist plots of Impedance and Electric Modulus in SLNBT ceramic suggest the relaxation to be non-Debye type. Imaginary parts of Impedance and Modulus vs. frequency at different temperatures are evaluated. The activation energies for the ac conductivity and relaxation times are calculated.

Keywords: Complex impedance spectroscopy, Electric modulus, Nyquist plots, Debye relaxations and AC conductivity.

1. INTRODUCTION

The layered perovskite materials are first studied by Aurivillius and are named after him as Aurivillius compounds. These compounds posses a structure [1-3] with general formula $(Bi_2O_2)^{2+}$ $(A_{n-1}B_nO_{3n+1})^{2-}$ where A is K^+, Ba^{2+}, Bi^{3+}etc, in twelve coordinated interstices and B is Ti^{4+}, Nb $^{5+}$, W^{6+},etc., which are octahedrally coordinated in perovskite layers, interleaved with $(Bi_2O_2)^{2+}$ layers [4] and n can be 1,2,3,4 and 5. Bismuth Layered Structured Ferroelectric (BLSF) ceramics can be made use of as piezoelectric sensors usable at high temperatures and at high frequencies, and as pyroelectric materials with large figures of merit [5,6]. BLSF's are characterized by (1) low dielectric constants (2) high curie temperatures and (3) large anisotropies in the electromechanical coupling factor K (K_{33}/K_{31}) as compared to widely used PZT ceramics [5]. Despite having evinced considerable interest in the potential for $Bi_4Ti_3O_{12}$ (BIT) being used as high temperatures piezoelectric sensors, pure BIT exhibits high dielectric loss is difficult to pole and is therefore not a suitable candidate for device fabrication. The addition of $SrCO_3$ to BIT results in materials which are considerably easier to pole and which exhibit excellent dielectric and piezoelectric properties [7].Complex Impedance Spectroscopy (CIS) is a very convenient and powerful experimental tool to correlate the structural and electrical characteristics in polycrystalline oxides in a wide range of frequencies. This helps to separate the contribution of electro active regions (such as grain boundary and bulk effects). CIS describes the electrical processes occurring in a system on applying an ac signal as input perturbation. The output response, when plotted in a complex plane plot, appears in the form of a succession of semicircles representing electrical phenomena due to the bulk material, grain boundary effect, and interfacial polarization. In view of the importance of ac impedance analysis, the present paper describes a detailed analysis of impedance and modulus studies which have been carried out in Lithium and Neodymium substituted Strontium Bismuth Titanate $Sr_{0.2}Li_{0.4}Nd_{0.4}Bi_4Ti_4O_{15}$ (SLNBT). No impedance and modulus analysis on SLNBT has been found in literature.

IJERT

2. EXPERIMENTAL

2.1 Processing method

Polycrystalline samples of SLNBT are prepared by conventional solid state reaction using high purity AR grade $SrCO_3$, Bi_2O_3, Li_2CO_3, Nd_2O_3 and TiO_2 powders in required stoichiometry. The powders are mixed thoroughly and calcined in air at 800^oC for 2h. The pellets are finally sintered at 1130^oC for 4h. Polyvinyl alcohol (PVA) is used as binder. The formation of compound is checked by X-ray diffraction technique. The sintered pellets are polished with fine emery paper in order to make both the surfaces flat and parallel. The pellets are then painted with silver paste for making electrical contacts and dried at 500^oC for 30 min. The impedance measurements are made over a wide range of frequency (20Hz-1MHz) at different temperatures (50^oC-600^oC) using Wayne Kerr 6500P LCR meter.

2.2 Impedance Parameters

Complex Impedance Spectroscopy is a well known and powerful technique which has been used for investigating dielectric materials. The contribution of various processes such as the electrode effects, bulk effects and the interfaces viz. the grain boundaries etc, can all resolved in the frequency domain. In general one or more of four representations are used to represent data in the complex plane [8].These are complex impedance (Z^*), complex admittance(Y^*), complex permittivity (ε^*) and complex modulus (M^*). All the four immittance functions are interrelated [9, 10].

$$Z^* = Z' - j Z'' \quad (1)$$
$$Y^* = Y' + j Y'' = j\omega C_0 \varepsilon^* \quad (2)$$
$$M^* = M' + j M'' = j\omega C_0 Z^* \quad (3)$$
$$\varepsilon^* = \varepsilon' - j \varepsilon'' \quad (4)$$

When the relaxation times of various processes differ as a consequence of different capacitive components, the complex impedance made use of. Alternatively complex modulus or plane plots are used to represent the response of dielectric system [11]. Complex impedance plane plots of real part of impedance (Z′) versus imaginary part of impedance (Z″) are useful in determining the dominant resistance of a sample. However, these are insensitive to smaller resistances. Similarly complex modulus plots are useful in determining the smallest capacitances. Sinclair and West [12] therefore suggested combined usage of impedance and modulus spectroscopic plots. The advantage of this technique is being that the M″ and Z″ peaks for a particular RC should be coincident on the frequency Scale (ideal Debye case). Hence the power of combined usage of impedance and modulus spectroscopy is that Z″ plot highlights phenomena with largest resistance where as M″ picks out those with smallest capacitances [13].

ISSN: 2278-0181
Vol. 2 Issue 6, June - 2013

3. RESULTS AND DISCUSSION

The X-ray diffractogram (XRD) of SLNBT is as shown infigure1.The XRD confirms the single phase formation.

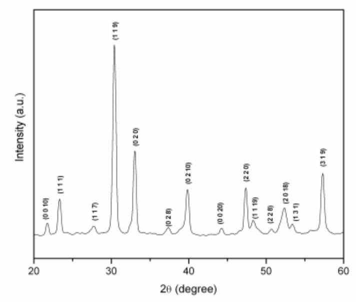

Fig.1. X-ray diffraction patterns of SLNBT

3.1 Complex Impedance Analysis

Figure 2 shows the temperature dependence of complex impedance spectrum (Nyquist plot) at selected temperatures. At lower temperatures the shape of the plot is a straight line with large slope indicating the insulating behavior of the sample. With the rise in temperature the slope the lines decreases and they bend towards real axis, at and above 400^{o}C. This shows that grain contribution in the sample at and above 400^{o}C. All semi circles exhibit some depression degree instead of a semi circle centered on the x-axis. This can be referred to as the non-Debye of relaxation in which there is a distribution of relaxation times. This non-ideal behavior can be co-related to several factors such as grain orientation, grain boundary, stress-strain phenomena and defect distribution. Figure 3(a) shows the variation of real part of impedance (Z′) with frequency at different temperatures. It is observed that the magnitude of Z′ decreases with increase in both frequency as well as temperature. This indicates reduction of grain, grain boundary and electrode interface resistances. The Z′ values for all temperatures merge above 100 kHz. This may be due to the release of space charges. The loss spectrum (i.e. Z″ versus frequency) of the compound at selected temperatures is given in figure 3(b). The asymmetric broadening of peaks suggests the presence of electrical process in the material with spread of relaxation time (indicated by peak width).The relaxation species may possibly be due to presence of electrons/species at lower temperatures and defects/vacancies at high temperatures[14,15]. The magnitude of existing peaks (Z″) decreases gradually with increase in frequency and temperature and finally merge in high frequency domain, which indicates the presence of space charge polarization effects at lower frequency and at higher temperature [16].

IJERT

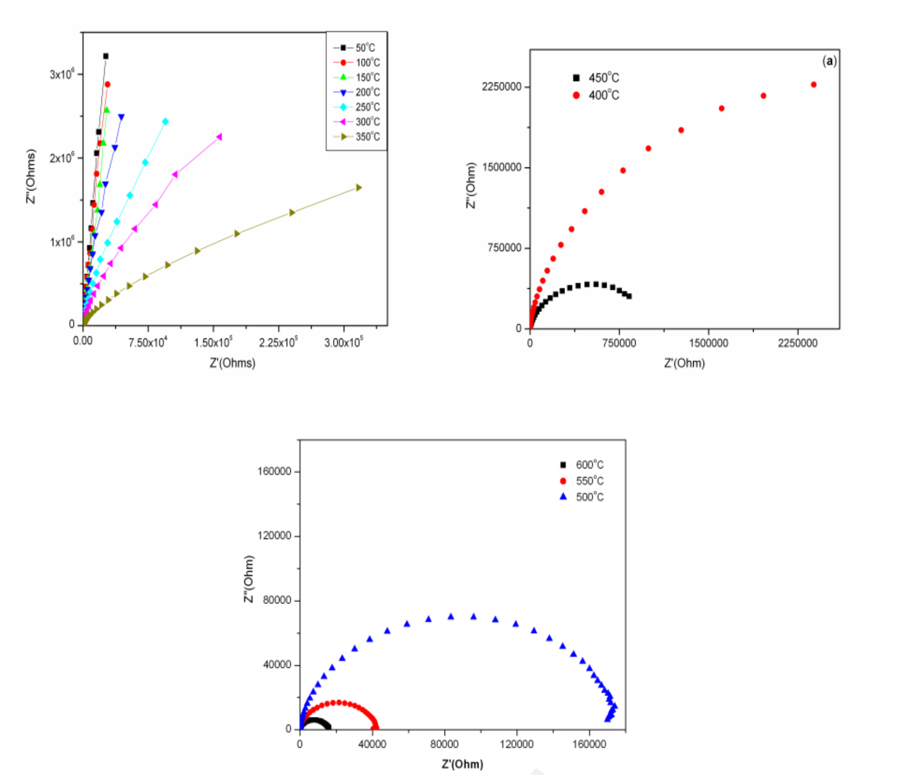

Fig.2. Complex impedence plos(Z'vs Z″) at selected temperatures

IJERT

Figure 4(a) shows the normalized imaginary part Z''/Z''_{max} of impedance as a function of frequency in SLNBT at selected temperatures. It is evident from the figure 4(a) that as the temperature increases the peak frequency of Z''/Z''_{max} shifts towards higher frequency side revealing that at high temperatures triggers another relaxation process. The Z''/ Z''_{max} parameter exhibit a peak with a slightly asymmetric degree at each temperature especially at high temperatures. At the peak relaxation defined by the condition

$$\omega\tau = 1 \tag{5}$$

Here τ is the relaxation time at peak.

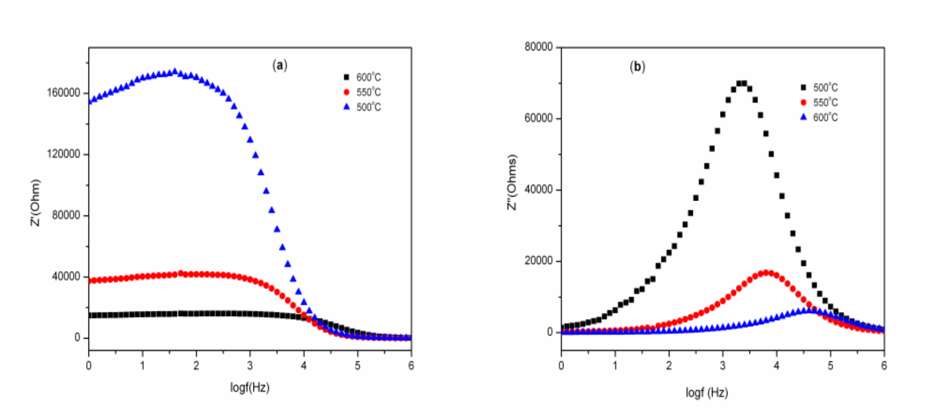

Fig.3.Frequency dependence of (a) real (Z'), (b) imaginary (Z") parts of impedance

Figure 4(b) shows the variation of relaxation time (logτ) with inverse of temperature (10^3/T). In a relaxation system, the relaxation time (τ) can be calculated from Z″ versus log f plot using relation

$$\tau = 1/\omega = 1/2\pi f_{max} \qquad (6)$$

Where, f_{max} is the relaxation frequency. It is observed that the value of τ found to be decreases with increase of temperature. The activation energy (E_a) of this compound has been calculated from Arrhenius relation

$$\tau = \tau_o \exp(-E_a/ k\,T) \qquad (7)$$

Where τ_o is the pre-exponential term, k is the Boltzmann's constant and T is the absolute temperature. The value of activation energy found to be 1.52eV.

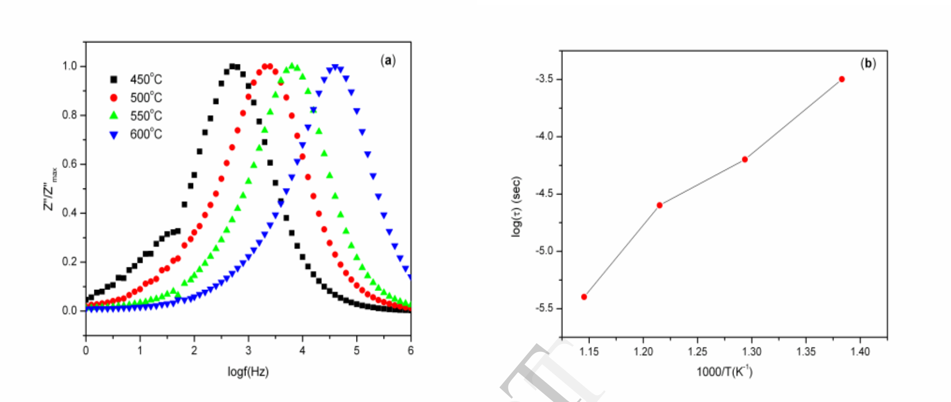

Fig.4 (a) normalized imaginary parts (Z"/Z"$_{max}$) of impedance as a function of frequency (b) Variation of relaxation time (log τ) versus 1000/T

IJERT

3.2 Modulus Spectrum Analysis

The advantage of adopting complex electric modulus formalism is that it can discriminate against electrode polarization and grain boundary conduction process. It is also suitable in detecting bulk phenomena properties as apparent conductivity relaxation times [12, 17]. The use of modulus spectroscopy plot is particularly useful for separating components with similar resistance but different capacitance. This complex modulus plots give complementary information to the information given by the impedance plots. The real and imaginary parts of electric modulus are obtained from the impedance data in accordance with the relations

$$M' = \omega\, C_0\, Z'' \qquad (8)$$

$$M'' = \omega\, C_0\, Z' \qquad (9)$$

where ω is angular frequency, C_0 is vacuum capacitance of the measuring cell and electrodes with an air gap in place of sample.

Figure 5(a) shows the variation of real part of electric modulus with frequency for SLNBT at different temperatures in the range 400-600^{o}C. For each temperature, M' reaches a constant value at high frequencies. At low frequencies, M′ reaches zero. Continuous dispersion on increasing frequency may be contributed to the conduction phenomena due to short range mobility of charge carriers. This implies the lack of a restoring force for flow of charge under the influence of a steady electric field [18].

Figure 5(b) shows the variation of imaginary part of electric modulus with frequency for SLNBT at different temperatures 400-600°C. The electrical modulus maxima (M''_{max}) shifts towards high frequency side with rise in temperature ascribing correlation between motions of mobile ions [19]. The asymmetric peak broadening shows that the relaxation is of non-Debye type which can be concluded due to the spreading of relaxation times with different time constant. The low frequency peaks shows that ions can move over long distances whereas, high frequency peaks merge to spatially confinement of ions in their potential well. The nature of modulus spectrum suggests the existence of hopping mechanism of electrical conduction in the material. The increase in peak (M″) value beyond 550° C due to dielectric phase transition around this temperature [20].

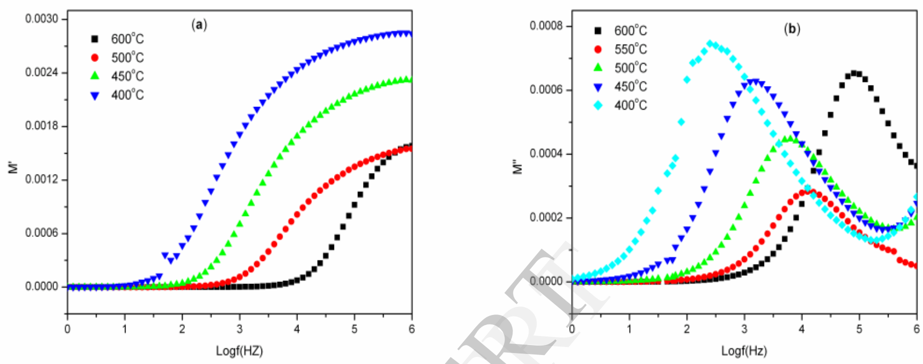

IJERT

Fig .5. (a) Real (M') and (b) imaginary (M") parts of electric modulus as a function of frequency at different temperatures

Figure 6(a) shows the complex electric modulus spectrum of SLNBT at selected temperatures. The patterns are characterized by depressed semicircular arcs whose centre does not lie on M′-axis. The behavior of electric modulus spectrum is suggestive of the temperature dependent hopping type of mechanism for electronic conduction in the system and non-Debye type dielectric relaxation. M′value decreases with temperature up to 550°C, beyond which the resistance started increasing due to dielectric transition near this temperature. Figure 6(b) shows the variation of relaxation time ($\log\tau_c$) with inverse of temperature ($10^3/T$). We derived the most probable conductivity relaxation times (τ_c) from peak frequency f_{max} in M" based on condition $2\pi f_{max}\,\tau_c = 1$. The activation energy found to be 1.45eV.Figure 7 shows the variations of Z″ and M″ with respect to frequency at 550°C. In ideal Debye behavior, the peaks should be coincident and the half height peak width 1.14 decades [17]. The magnitude of M″ is lower than the magnitude of Z″, shows the non Debye behavior.

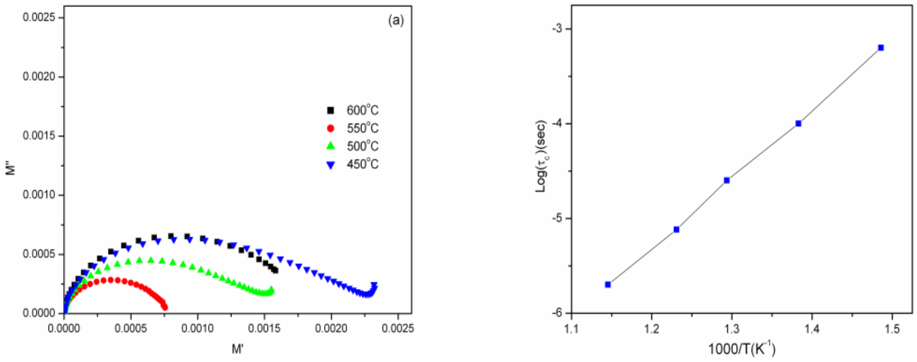

Fig. 6 (a) Complex electric modulus plots (M" vs. M') at selected temperatures. (b) Variation of relaxation time (log τ) with inverse of temperature 10^3/T

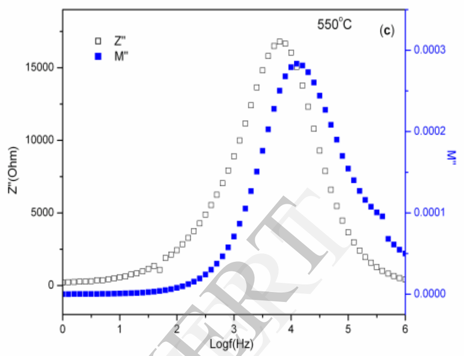

Fig.7. Variation of Z" and M" with frequency at 550°C

3.3 AC Conductivity: The ac conductivity is calculated from impedance data using the relation

$$\sigma' = Y' (t/A) \tag{10}$$

Where σ' and Y' are the real parts of ac conductivity and admittance (Y*=1/Z*) respectively, t is thickness and A is area of pellet. Figure 8 represents the variation of real part of ac conductivity with temperature. It is observed that in the low temperature region there is a distinct dispersion in the values of conductivity. In the high temperature region, the dispersion decreases due to intrinsic conductivity at these temperatures. The variation profile shows the Negative Temperature Coefficient of Resistance (NTCR) behavior of SLNBT. The activation energy for conduction is determined using the Arrhenius relationship

$$\sigma_{ac} = \sigma_0 \exp(-E_{ac}/KT) \tag{11}$$

Where σ_0 is pre-exponential term, E_{ac} is activation energy for conduction, K is Boltzmann's constant and T is absolute temperature. A linear least square fitting of the conductivity data to equation (11) gives the value of activation energy (E_{ac}). The values of activation energies in temperature region 400-600°C are given in table (1). The activation energy decreases with increase in frequency. Here hopping of charge carriers comes into picture. The power law [21] dependence of ac conductivity on high frequency ($\sigma_{ac} = f^{\,n}$, where n is function of temperature as well as frequency) is of universal nature, and corresponds to short range of hopping of charge carriers through the trap sites separated by energy barriers of varied heights. Since temperature is high enough for the band to band transition to dominate the conduction process, n becomes almost zero because electronic conduction is frequency independent. The ac conductivity vs. frequency curves for different sample temperature converges with one another at high frequency. This indicates that at high frequencies the ac conduction becomes almost independent of temperature. This might be one of the reasons that at high frequencies the activation energy calculated from ac conductivity curves are less than at lower frequencies [22, 23].

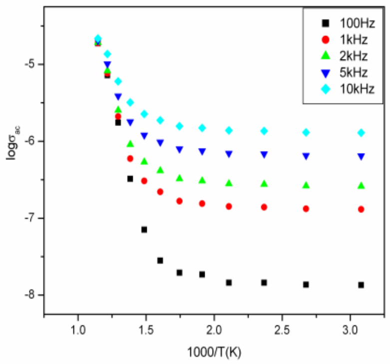

Fig.8. Arrhenius plot of ac conductivity.

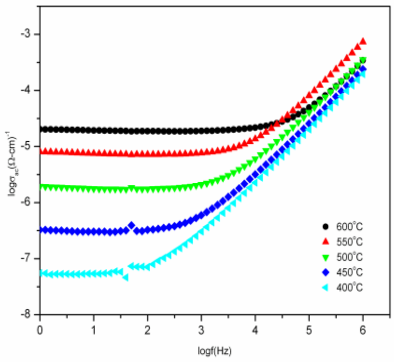

Fig.9. Frequency dependency of ac conductivity

IJERT

TABLE1. AC conductivity activation energies at different frequencies in the temperature region 400-600^{o}C

Frequency	Activation energy(eV)
100 Hz	1.44
1 kHz	1.08
2 kHz	0.94
5 kHz	0.74
10 kHz	0.60

Figure 9 shows the real part of ac conductivity of the sample as a function of frequency at selected temperatures. It appears that, in low temperature region the ac conductivity depends significantly on frequencies and it is usually observed in this type of materials [24]. With the increase in temperature the dielectric relaxation takes place and dependence of conductivity on frequency gets modified. The conductivity at 550^{o}C is high in high frequency region. 550^{o}C is Curie temperature of this sample, due to this high conductivity.

4. CONCLUSIONS

Polycrystalline sample of SLNBT is prepared by high temperature solid state reaction method and phase formation is confirmed by XRD. The asymmetric semicircles of Nyquist plot suggest non-Debye type relaxations in the system. Shifting of Z″ maxima and M''_{max} to higher frequency side with increase of frequency indicates the temperature relaxation process in the material. NTCR is observed from ac conductivity studies of SLNBT. The activation energies are decreased with increase of frequency.

ACKNOWLEDGEMENTS

The authors thank Board of Research in Nuclear Sciences (BRNS) for providing financial support and the Management, Vardhaman College of Engineering for constant encouragement.

REFERENCES

[1] B.Aurivillius, Ark. Kemi 1, (1949) 463-480.
[2] B.Aurivillius, Ark. Kemi 1, (1949) 499-512.
[3] B.Aurivillius, Ark. Kemi 1, (1950) 519-527.
[4] E. C. Subbarao,J. Phys. Chem. Solids 23, (1962) 665-676.
[5] T. Takenaka, K. Sakata, J. Appl. phys. 55, (1984) 1092-1099.
[6] H. S. Schulman, M.Testorf, Damjanovic & N. Setter, J. Am. Ceram. Soc. 79, (1996) 3124-3128.
[7] S. Ikegami and I. Ueda, Jpn. J. Appl. Phys., Part 1, 13, (1974) 1572-1577.
[8] H. J. De Bruin, S.P.S. Badwal, J. Aust. Ceram. Soc., 14, (1978) 20-28.
[9] D.C. Sinclair and A.R. West, J.Appl.phys. 8, (1986) 66
[10] K. Srinivas, P. Sarah and S. V. Suryanarayana, Bull.Mater.Sci. 26(2), (2003) 247-253.
[11] S. P. S. Badwal, proceedings of the international seminar on solid state Ionic Devices, World Scientific Publishing, Singapore, 1988, p.165.
[12] D.C. Sinclair and A.R. West, J.Appl.phys. 66(8), (1989) 3850-3857.
[13] D.C. Sinclair and A.R. West, J.Mater.Sci. 29, (1994) 6061-6068.
[14] A. Laha and S.B. Krupanidhi, Solid State Commun. 127, (2003) 247
[15] P. S. Sahoo, A. Panigrahi, S. K. Patri and R. N. P. Choudary, J.Mater. Sci: Mater Electron. 20, (2009) 565-570.
[16] S.Dutta, P.K.Sinha, and R. N. P. Choudary, J. Appl. phys. 96, (2004) 1607-1613.
[17] I. M. Hodge, M. D. Ingram, A.R. West, J.Electroanal.Chem. Interfacial Electrochem. 74, (1976) 125-143.
[18] P.B. Macedo, C.T. Moynihan, R. Bose, Phys.Chem. Glasses, 13, (1972) 171-179.
[19] F.Borsa, D.R. Torgeson, S.W. Martin, H.K. Patel, Phys. Rev. B46, (1992) 795.
[20] K. Sambasiva Rao, D. Madhava Prasad, P. Murali Krishna and T.Swarna Latha, Ceramics-Silikaty.52 (3), (2008) 190-200.
[21] A.K.Jonscher, Nature.267, (1977) 673.
[22] S.Bhattacharya,S.Bharadwaja, and S.B. Krupanidhi, J. Appl. phys. 88, (2000) 1.
[23] K. Prabakar, S. K. Narayanadass, and D. Mangalaraj,Cryst. Res. Technol. 37, (2002) 1094
[24] R. Rizwana, T. Radha Krishna, A. R. James, and P.Sarah, Cryst.Res.Technol.42, 7 (2007) 699-706.

IJERT